Optical Properties and Thin Film Processing of Nickel Phthalocyanine Nanoparticles Prepared by Laser Ablation in Liquid

Yuchun Wang, Hiroyuki Wada

[1]*Institute of Science Tokyo, Japan*
[*]*Corresponding author's e-mail: wada.h.ac@m.titech.ac.jp*

Nickel phthalocyanine (NiPc) nanoparticles were synthesized by laser ablation in liquid (LAL). The particle size, morphology, and optical properties were controlled by adjusting the laser fluence and irradiation time. SEM and DLS analyses indicated that higher laser fluence and irradiation time promoted the formation of smaller and more uniform nanoparticles. UV–Vis spectroscopy confirmed that the characteristic Q-band absorption of NiPc remained after laser processing, indicating that the molecular structure remained stable. The nanoparticles were transferred into chloroform and deposited as thin films by spin coating. Film thickness and optical absorbance increased with deposition volume, while surface morphology remained consistent. This work demonstrates a controllable, surfactant-free approach to producing NiPc nanoparticle thin films with stable optical properties, offering potential for future solution-processed optoelectronic applications.
DOI: 10.2961/jlmn.2026.02.2008
Keywords: Nickel phthalocyanine; Laser ablation in liquid; Nanoparticles; Thin films; UV-Vis spectroscopy; Spin coatings

1. Introduction

Organic semiconductors have attracted significant attention due to their structural tunability, solution processability, and optoelectronic properties [1-3]. Among organic semiconductors, phthalocyanines (Pc) are a family of two-dimensional, macrocyclic compounds consisting of four isoindole groups connected by nitrogen atoms and containing an extended π-conjugated system. Coordination of different metal ions creates metallophthalocyanines (MPcs), which affect their properties and enable the tuning of material performance for various applications [4,5]. Pc-based thin films have been studied in a wide range of fields, including chemical sensing [6], nonlinear optics [7], electrocatalysis [8], biomedical imaging [9], and optoelectronic devices such as photovoltaics and field-effect transistors [10], owing to their strong visible–NIR absorption, high thermal and chemical stability, and good carrier transport abilities [4,11,12].

Despite these benefits, the practical application of phthalocyanines in solution processing is currently limited. Their low solubility in most traditional solvents, coupled with a high tendency to aggregate, inhibits stability of dispersion and makes film deposition difficult [12-14]. As a result, all these problems limit the applicability in solution-based device fabrication.

To overcome these limitations, the conversion of phthalocyanines into nanoparticles has become one of the promising methods of enhancing dispersion stability and processability. Particle size reduction enhances colloidal stability and helps in the development of uniform films [15]. Several routes have also been investigated for phthalocyanine nanoparticle synthesis, i.e., precipitation, surfactant-assisted assembly, and solvent-based techniques. Most of the reported techniques, however, incorporate complicated processing protocols or the use of chemical additives, which compromise the material's quality and compatibility in device processing [16-18].

Laser ablation in liquid (LAL) provides a high-quality, top-down, and surfactant-free approach for the synthesis of nanoparticles. In this method, a pulsed laser is irradiated onto a solid or powdered target suspended in a liquid medium, and the rapid localized heating and ablation of material form nanoparticles. During the synthesis process, particle morphology and optical properties can be controlled by adjusting laser fluence and irradiation time [19-22]. The preparation of surfactant-free nickel phthalocyanine nanoparticles by LAL could offer a solution to stable dispersion and film-quality issues while preserving the optoelectronic properties of the material.

In this study, NiPc nanoparticles were synthesized by LAL and characterized for their morphology and optical properties. The nanoparticles were then deposited into thin films by the spin-coating method, and the effects of spin-coating parameters on film quality were investigated. This work presents a surfactant-free, controllable method to produce NiPc nanoparticles and the corresponding thin films for future photovoltaic applications.

2. Experimental Procedures

Nickel Phthalocyanine (NiPc) nanoparticles were synthesized by Laser Ablation in Liquid. NiPc powder (Sigma-Aldrich) was dispersed in 20 mL of deionized water by sonicating for 10 min to get uniform dispersion. The dispersion was placed in a square glass bottle on a magnetic stirrer rotating at 500 rpm to ensure even exposure during laser irradiation. The pulsed Nd:YAG laser (532 nm, 13 ns , 10 Hz) was irradiated horizontally into the liquid with a beam spot

size of approximately 0.5 cm². The laser generated localized heating, which fragmented the NiPc into nanoparticles. Although NiPc exhibits stronger absorption at shorter wavelengths, laser ablation in liquid is not only induced by linear optical absorption. Under the high fluence conditions used in this study, nonlinear processes such as multiphoton absorption can imduce effective material fragmentation at 532 nm. The preservation of the characteristic Q-band in the UV-Vis spectra also indicates that the molecular structure remains stable after laser irradiation. After laser ablation, the dispersion was centrifuged (3000 rpm, 20 min) to remove large unablated fragments and aggregated particles, ensuring a more homogeneous and stable dispersion for characterization and thin film fabrication. It should be noted that centrifugation can influence the particle size distribution. Therefore, the DLS results mainly represent the size of the stable colloidal particles rather than the entire sample prepared by LAL. Since all samples were processed under the same centrifugation conditions, the observed trends are still meaningful for comparing the effects of laser fluence and irradiation time. No surfactants or stabilizers were used in this process, ensuring the purity of the nanoparticles for further analysis and thin film deposition.

To investigate the effect of laser conditions on particle properties, the laser fluence was varied from 125 to 500 mJ/cm² and irradiation time from 15 to 60 minutes. The morphology, particle size distributions, and optical properties of the produced nanoparticle dispersions were examined by scanning electron microscopy (SEM), dynamic light scattering (DLS), and UV-Vis spectroscopy, respectively. The optimized nanoparticle dispersions were then used to produce thin films.

To determine a suitable solvent for film processing, the solubility of unprocessed NiPc powders was tested in chloroform, hexane, and toluene. Chloroform had the highest solubility and was therefore chosen as the solvent for the spin-coating test. After laser ablation, the NiPc nanoparticle supernatant was collected by centrifugation and the mixture was stirred overnight using the solvent exchange method to transfer the nanoparticles from the water phase to the chloroform phase. The chloroform-based nanoparticle dispersion was spin-coated onto a glass substrate previously washed with deionized water, ethanol, and isopropanol to fabricate thin films. The spinning speed and duration were always kept constant (1000 rpm, 60 s)while the volume of the dispersion varied between 0.1 and 0.3 mL. The light absorption, surface morphology, and thickness of the films were evaluated using UV-Vis spectroscopy, atomic force microscopy (AFM), and Dektak profilometer, respectively, to determine the quality and properties of the films.

3. Results and Discussion

Scanning electron microscopy (SEM) was used to observe the morphology of nanoparticles synthesized by the laser ablation in liquid (LAL) method under different laser conditions. As shown in Figure 1, most particles exhibit irregular shapes at lower laser fluence and shorter irradiation times. However, with increasing fluence and irradiation time, an increasing number of particles show more rounded shapes with smoother edges and more uniform outlines. This phenomenon can be explained by the laser melting in liquid (LML), in which local heating by laser irradiation caused the melting of the material fragments. Surface tension reshapes the melting particle to a round or spherical shape with minimum surface energy. [23-25] The coexistence of irregular and more rounded particles may be caused by the combined effects of laser-induced fragmentation and localized thermal processes during nanosecond pulsed irradiation. In this process, the energy distribution within the laser spot is not perfectly uniform, which may lead to different morphologies of the particles, resulting in the simultaneous formation of fragmented and partially reshaped particles. At the lower fluence (125 mJ/cm²) and shorter irradiation time (15 minutes), many large, irregular, unablated raw material remained in the sample, indicating incomplete ablation. As the fluence increased to 500 mJ/cm², and the irradiation time extended to 60 minutes, the SEM images showed more nanoparticles with round shapes, and the remaining large fragments were significantly reduced. These observations indicate that both laser fluence and irradiation time play an important role in controlling particle morphology through a combination of thermal ablation and melting dynamics.

Dynamic light scattering (DLS) was used to evaluate the secondary particle size. DLS measurements were performed

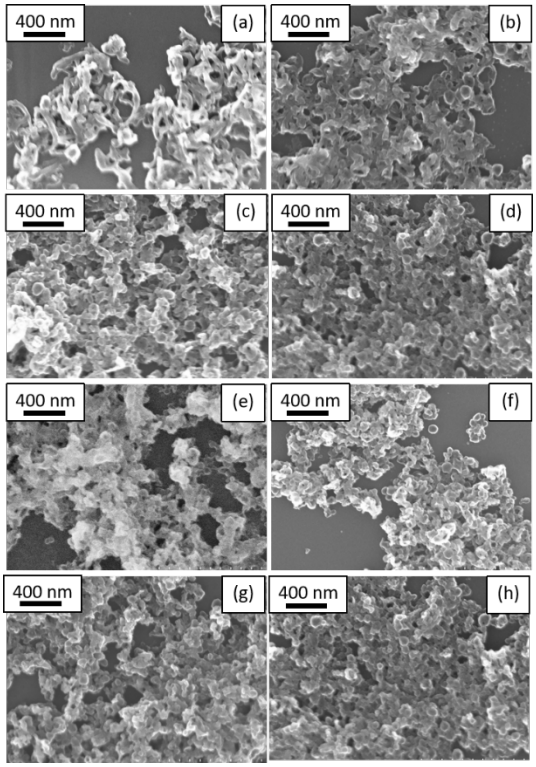

Fig. 1 SEM images of NiPc nanoparticles synthesized under varying laser parameters. (a–d) Fluence-dependent morphology at a fixed irradiation time of 30 minutes (125, 250, 350, and 500 mJ/cm², respectively). (e–h) Irradiation time-dependent morphology at a constant fluence of 500 mJ/cm² (15, 30, 45, and 60 minutes, respectively).

at 25 ℃. The samples were measured after centrifugation without further modification, using standard automatic acquisition settings. Since all samples were subjected to identical centrifugation conditions, the DLS results mainly reflect the stable colloidal fraction after removal of large aggregates and unablated fragments. As shown in Figure 2, the secondary particle size decreased with increasing laser

fluence, the size distribution also became narrower, indicating improved size uniformity at higher fluences. A similar tendency was observed when the irradiation time increased at a fixed fluence of 500 mJ/cm². When the irradiation time was extended from 15 to 60 minutes, the particle size decreased. These results suggest that both laser energy and duration contribute to more efficient particle fragmentation. Complete DLS size distributions for all fluence and irradiation time conditions are provided in Supplementary Figure S1.

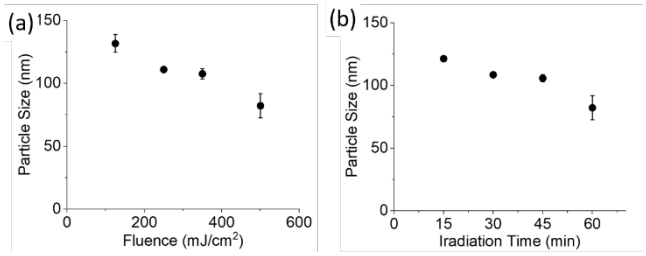

Fig. 2 Secondary particle size of NiPc nanoparticles as a function of (a) laser fluence and (b) irradiation time, measured by DLS.

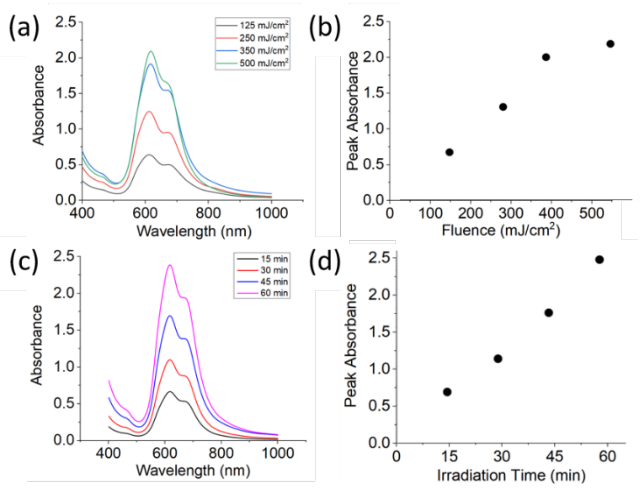

Fig. 3 (a) UV-Vis spectra of NiPc nanoparticles at fluences of 125–500 mJ/cm² (60 minutes);(b) Peak absorbance at 618 nm vs. fluence;(c) UV-Vis spectra at irradiation times of 15–60 minutes (500 mJ/cm²);(d) Peak absorbance at 618 nm vs. time.

Figure 3 presents the UV-Vis absorption spectra of NiPc nanoparticle dispersions synthesized under various laser fluence and irradiation times. All the samples showed a characteristic splitting Q-band with two absorption peaks at around 618 nm and 668 nm. These peaks correspond to π–π* transitions within the phthalocyanine ring structure and are consistent with spectral features of NiPc in literature. [26,27] With increasing laser fluence from 125 to 500 mJ/cm², the absorbance increases significantly, indicating enhanced ablation and a higher yield of nanoparticles. A similar trend is observed with increasing irradiation time from 15 to 60 minutes, where longer irradiation time leads to higher absorbance. This increase in absorbance is mainly attributed to a higher concentration of NiPc dispersed in the colloidal phase, resulting from more efficient laser ablation. This behavior reflects the total energy input of the laser process, which promotes more effective ablation and dispersion of NiPc into smaller, colloidally stable particles. The position and shape of the peaks remain stable under all laser conditions, indicating that the LAL process did not change the optical properties of NiPc. No significant peak shifting was observed, indicating that no major chemical reaction or degradation occurred during the laser ablation process.

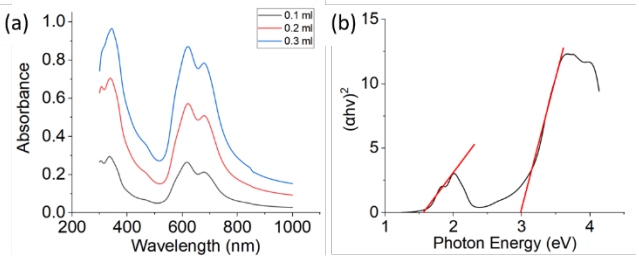

Fig. 4 (a) UV-Vis absorption spectra of NiPc thin films spin-coated using 0.1, 0.2, and 0.3 mL of dispersion. (b) Tauc plot of the 0.3 mL NiPc thin film.

Figure 4a shows the UV-Vis absorption spectra of NiPc films prepared by spin-coating 0.1, 0.2, and 0.3 mL chloroform dispersions of NiPc nanoparticles on glass substrates. All the samples show the splitting Q-band peaks at around 618 nm and 668 nm, and B-band below 400 nm. Increasing the deposition volume leads to an increase in absorbance, which indicates improved coverage and thickness of the films. These results suggest that adjusting the spin-coating volume directly affects the absorbance and thickness of the resulting NiPc films, which is crucial for photovoltaic applications. To estimate the optical band gap, a Tauc plot based on a direct allowed transition model was constructed using the absorption data from the 0.3 mL film. (Figure 4b) The estimated band gap values were 1.57 eV for the Q-band and 2.98 eV for the B-band. These values are consistent with those reported for other metallophthalocyanines. [27-29] The presence of both Q- and B-band absorption confirmed that the electronic structure of NiPc maintained stability, and the resulting band gap energies placed the material among the class of low band gap organic semiconductors. These findings support the potential of laser-synthesized NiPc nanoparticles for optoelectronic thin film applications.

The surface morphology of NiPc films prepared using different deposition volumes (0.1, 0.2 and 0.3 mL) was characterized by atomic force microscopy (AFM). The AFM images in Figure 5 show consistent grain features across all samples, indicating that thin films were formed by densely packed NiPc nanoparticles. The 2D and 3D AFM images show relatively similar surface textures across the samples, indicating that changes in deposition amount have a minor effect on the nanoscale surface roughness. Film thickness was tested by Dektak profilometer. The average thicknesses of the films prepared with 0.1, 0.2, and 0.3 mL were 115.0 nm, 131.5 nm, and 173.5 nm, respectively. The thickness increased with increasing deposition sample volume, which correlated with the absorbance intensity observed in the UV-Vis spectra. These results indicate that although the morphology and surface structure of the nanoparticles remain consistent, the film thickness can be effectively controlled by adjusting the spin-coating volume.

4. Conclusion

In this work, nickel phthalocyanine (NiPc) nanoparticles were successfully prepared by laser ablation in liquid (LAL)

method. By changing laser fluence and irradiation time, the

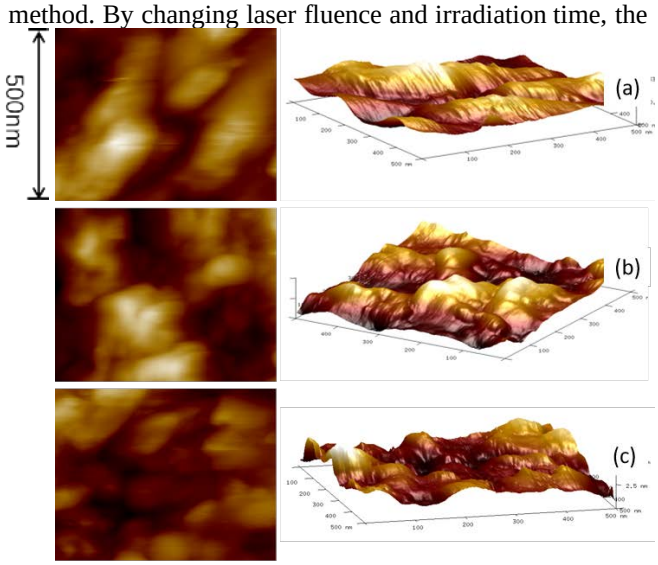

Fig. 5 (d) n-coated persions. ktak pro-

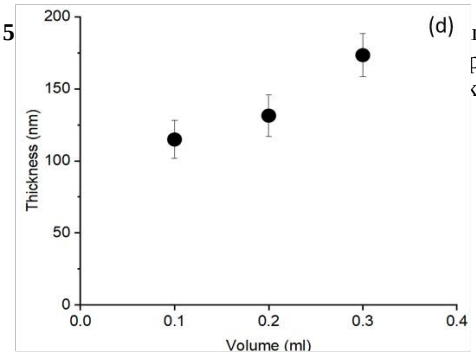

morphology and optical properties of nanoparticles could be controlled. SEM and DLS analysis indicated that higher laser fluence and longer irradiation time promoted the formation of smaller nanoparticles with higher yield. UV-Vis spectroscopy showed the characteristic splitting Q-band absorption peaks of NiPc after laser processing, indicating that the molecular structure remained stable. The prepared nanoparticles were transferred to chloroform and used to fabricate thin films by spin coating. Film quality was evaluated through UV-Vis spectroscopy, AFM, and Dektak profilometry, showing that film thickness and optical density could be controlled by changing deposition volume. These results indicate that the LAL method achieved controllable synthesis and thin-film integration of NiPc nanoparticles without chemical additives.

This work shows promise for the potential of phthalocyanine nanoparticles prepared by LAL for future use in solution-processable optoelectronic devices. Future work will focus on device fabrication and functional performance evaluation.

Acknowledgments

The authors thank Prof. Kitamoto for providing access to DLS and SEM measurements, and Dr. Kajitani and the Open Facility Center for assistance with AFM and Dektak profilometry at Institute of Science Tokyo.

References

[1] M. Riede, B. Lüssem, and K. Leo: "Comprehensive Semiconductor Science and Technology, Vol. 4" ed. by P. Bhattacharya, R. Fornari, and H. Kamimura, (Elsevier, Amsterdam, 2011) p. 448.
[2] H. Sirringhaus: Adv. Mater., 26, (2014) 1319.
[3] T. Okamoto, R. Komatsu, S. Nishimura, M. Unno, K. Isogai, M. Nakano, and K. Takimiya: Sci. Adv., 6, (2020) eaaz0632.
[4] V. Coropceanu, J. Cornil, D.A. da Silva Filho, Y. Olivier, R. Silbey, and J.L. Brédas: Chem. Rev., 107, (2007) 926.
[5] W. Wu, Y. Liu, and D.B. Zhu: Chem. Soc. Rev., 39 (2010) 1489.
[6] R. Ridhi, G. Saini, and S.K. Tripathi: Mater. Res. Express, 4, (2017) 025027.
[7] K. Kumagai, G. Mizutani, H. Tsukioka, T. Yamauchi, and S. Ushioda: Phys. Rev., B 48, (1993) 14488.
[8] J. Zagal, M. Páez, A.A. Tanaka, J.R. dos Santos Jr., and C.A. Linkous: J. Electroanal. Chem., 339, (1992) 13.
[9] Y. Wang and H. Wada: J. Laser Micro Nanoeng., 18, (2023) 2004.
[10] O.A. Melville, B.H. Lessard, and T.P. Bender: ACS Appl. Mater. Interfaces, 7, (2015) 13105.
[11] G. de la Torre, C.G. Claessens, and T. Torres: Chem. Commun., 20, (2007) 2000.
[12] N. Karl: Synth. Met., 133–134, (2003) 649.
[13] L.P. Gergely, Ç. Yüceel, Ü. İşci, F.S. Spadin, L. Schneider, B. Spingler, M. Frenz, F. Dumoulin, and M. Vermathen: Mol. Pharm., 20, (2023) 4165.
[14] Y. Chin, S.H. Lim, Y. Zorlu, V. Ahsen, L.V. Kiew, L.Y. Chung, F. Dumoulin, and H.B. Lee: PLoS One, 9, (2014) e97894.
[15] T. Furuyama, K. Satoh, T. Kushiya, and N. Kobayashi: J. Am. Chem. Soc., 136, (2014) 765.
[16] J. Neddersen, G. Chumanov, and T.M. Cotton: Appl. Spectrosc., 47, (1993) 1959.
[17] H. Imam, K. Elsayed, M.A. Ahmed, and R. Ramdan: Opt. Photonics J. 2 (2012) 11.
[18] D. Zhang, B. Gökce, and S. Barcikowski: Chem. Rev., 117, (2017) 3990.
[19] D. Zhang, Z. Li, and K. Sugioka: J. Phys. Photonics, 3 (2021) 042002.
[20] W. Borzęcka, A. Domiński, and M. Kowalczuk: Nanomater., 11, (2021) 2426.
[21] A.M. Schmidt and M.J.F: Molecules, 26 (2021) 2823.
[22] J.F. Lovell, C.S. Jin, E. Huynh, C. Kim, J.L. Rubinstein, W.C.W. Chan, W. Cao, L.V. Wang, and G. Zheng: Nat. Mater., 10, (2011) 324.
[23] Y. Ishikawa, T. Tsuji, S. Sakaki, and N. Koshizaki: Prog. Mater. Sci. 131, (2023) 101004.
[24] H. Usui, Y. Shimizu, T. Sasaki, and N. Koshizaki: J. Phys. Chem. B, 109, (2005) 120.
[25] L. Liang, Y. Shimizu, M. Masuda, T. Sasaki, and N. Koshizaki: J. Phys. Chem. C, 123, (2019) 24934.
[26] M.M. El-Nahass, K.F. Abd-El-Rahman, and A.A.A. Darwish: Mater. Chem. Phys., 92, (2005) 185.
[27] B. Joseph and C.S. Menon: J. Thin Film Sci. Tec., 4, (2007) 255.
[28] K.J. Hamam and M.I. Alomari: Appl. Nanosci., 7, (2017) 261.
[29] T. Hussein, E.M. Nasir, A.H. Al-Aarajiy: Int. J. Thin Film Sci. Tec., 1, (2012) 71.

(Received: January 8, 2026, Accepted: May 16, 2026)